

A MAGNETICALLY-SWITCHED, ROTATING BLACK HOLE MODEL
FOR THE PRODUCTION OF EXTRAGALACTIC RADIO JETS AND THE
FANAROFF AND RILEY CLASS DIVISION

D. L. MEIER

Jet Propulsion Laboratory, California Institute of Technology, Pasadena, CA 91109

Submitted to The Astrophysical Journal.

ABSTRACT

A model is presented in which both Fanaroff and Riley class I and II extragalactic jets are produced by magnetized accretion disk coronae in the ergospheres of rotating black holes. It employs a hybrid version of the Blandford-Payne and Blandford-Znajek magnetohydrodynamic mechanisms (similar to the Punsly-Coroniti model, with the addition of a metric-shear-driven dynamo) and a generalized form of the magnetic switch, which is shown to be the MHD analog of the Eddington luminosity. While the jets are produced in the ergospheric accretion disk itself, the output power still is an increasing function of the black hole angular momentum. For high enough spin, the black hole triggers the magnetic switch, producing highly-relativistic, kinetic-energy-dominated jets instead of magnetic-energy-dominated ones for lower spin. The coronal mass densities needed to trigger the switch at the observed FR break power are quite small ($\sim 10^{-15} \text{ g cm}^{-3}$), implying that the source of the jet material may be either a pair plasma or very tenuous electron-proton corona, not the main accretion disk itself.

The model explains the differences in morphology and Mach number between FR I and II sources and the observed trend for massive galaxies (which contain more massive black holes) to undergo the FR I/II transition at higher radio power. It also is consistent with the energy content of extended radio lobes and explains why, because of black hole spindown, the space density of FR II sources should evolve more rapidly than that of FR I sources.

A specific observational test is proposed to distinguish between models like this one, in which the FR I/II division arises from processes near the black hole, and models like Bicknell's, in which the difference is produced by processes in the host galaxy's interstellar medium. If the present model is correct, then the ensemble average speed of parsec-scale jets in sources distinguished by their FR I *morphology* (not luminosity) should be distinctly slower than that for sources with FR II morphology. The model also suggests the existence of a population of high-redshift, sub-mJy FR I and II radio sources associated with spiral or pre-spiral galaxies that flared once when their black holes were formed but were never again re-kindled by mergers.

Subject headings: black hole physics — galaxies: jets — galaxies: nuclei — hydrodynamics — MHD — quasars: general — radio continuum: galaxies — relativity

1. INTRODUCTION

Recently many authors have pointed out that the speeds of jets associated with different types of compact object (pre-main-sequence star, white dwarf, neutron star, black hole) are approximately equal to the Keplerian or escape speed from the surfaces of those compact objects. However, some caution must be exercised in taking this equivalence too literally. A good example of this is the extragalactic radio source class. All are believed to be powered by accretion onto black holes, from whose surface (the horizon) the escape velocity is exactly c , the speed of light. However, while all extragalactic jets appear to be at least mildly relativistic, the speeds obtained from Very Long Baseline Interferometry (VLBI) observations range from $\beta_j \equiv v_j/c \sim 0.1$ in Centaurus A (Tingay et al. 1998) to $\gamma_j \equiv (1 - \beta_j^2)^{-1/2} \sim 10$ in 3C 345 (Vermeulen 1996). In terms of the proper velocity $u_j = \gamma_j \beta_j$, this represents a range of two orders of magnitude in jet speed. Clearly, even before traversing the main part of the interstellar medium, jet speeds are strongly affected by the details of the acceleration and collimation process near or in the accreting black hole system.

Radio jets on the kiloparsec scale also differ dramatically in speed, and these differences apparently translate into a morphological difference. Subsonic or transonic jets with velocities less than $\sim 0.6c$ are believed to be responsible for producing the Fanaroff and Riley Class I sources (Fanaroff & Riley 1974; Bicknell 1985; Bicknell 1995). The FR I sources are distinguished by generally low radio power, often complex morphology (S-shaped, C-shaped, *etc.*), and diffuse lobes that have their bright region close to the associated galaxy — all consistent with transonic flow that decelerates into subsonic flow. Class II sources generally are much more powerful, have only a straight morphology, and have their brightest point at the far ends of the dumbbell-shaped source. They are thought to be produced by highly supersonic jets that terminate in a strong shock where the high-speed flow strikes the interstellar medium.

A mechanism for determining the speed of jets at their site of acceleration was suggested by Meier et al. (1997a), hereinafter MEGPL. Termed the “magnetic switch” because of the two distinct slow and fast jet states, this mechanism operates in the magnetized corona of the black hole accretion disk itself. Fast (highly relativistic) jets are produced when the coronal plasma is unbound by the mag-

netic field, and slow (trans-relativistic) jets at roughly the disk escape velocity are produced when the corona is initially bound. This simple physical process is a good candidate for explaining the difference between the two Fanaroff & Riley classes, because it explains how jets with radically different speeds could occur in otherwise similar sources. However, as discussed in section 2 below, the magnetic switch, triggered solely by the magnetic field strength (or even by coronal density), fails to explain why these morphological differences have rather long lifetimes (10^{6-7} yr).

One way out of this dilemma is to assume that all radio jets for a given galaxy mass indeed do start out in the nucleus with about the same average speed, but, depending on local galaxy properties (which do have long lifetimes), are affected differently by deceleration processes in the interstellar medium (Bicknell 1995). Indeed, jet deceleration *has* been inferred from variations in the jet-to-counterjet ratio in observations of FR I sources (Laing 1996). In this paper, however, we propose an alternate method for maintaining long-lived FR I or FR II morphology — one that preserves the magnetic switch model, along with all of its attractive properties, and suggests a reason *why* some jets may be more prone to deceleration than others. Since the power in these MHD outflows also depends on the angular velocity of the magnetic field, *it is suggested that the difference in radio power among galaxies of the same mass is due to different magnetic field rotation rates in their central engine, caused by different spin rates of their central black holes.* This has been suggested before (Baum, Zirbel, & O’Dea 1995) based on observations alone, but this paper derives such a behavior directly from a generalized theory of the magnetic switch. As we show below, black holes of different spin should produce jets of different power and velocity, and a sharp FR I/II-like transition is expected to occur. Unlike the ISM model, this model predicts a different mean jet velocity in the central parsec for the FR I and FR II classes, yielding a definite observational test for distinguishing between the two.

Note that the magnetically-switched, rotating black hole model depends critically on the jet luminosity being a direct function of the black hole angular momentum — in direct conflict with the conclusions of Livio, Ogilvie, & Pringle (1999). Therefore, section 3.2 spends some time on this issue and shows that, while the basic tenets of these authors are correct, nevertheless, if the accretion disk within the ergosphere is taken into account, a Blandford-Znajek-like (BZ) expression for the jet power is recovered — even though the jet is ejected from the accretion disk itself by a Blandford-Payne-like (BP) mechanism. The jet production model is similar to the Punsly-Coroniti (PC) ergospheric wind mechanism (Punsly & Coroniti 1990b). Furthermore, due to an expected *metric-shear-driven* dynamo (see the Appendix), the poloidal magnetic field in the ergosphere is expected to have a larger value than that suggested by Livio, Ogilvie, & Pringle (1999), leading to radio jet powers comparable to those observed.

The outline of the paper is as follows. Section 2 briefly reviews the classical magnetic switch model and the reasons for its failure to explain the FR I/II break. Section 3 presents the generalized magnetic switch (including rotation as a parameter) and its role in the rotating black hole model for jet production and for the FR I/II transition. Section 4 discusses applications of the model to re-

cent observations of radio sources, with observational and theoretical tests of the model proposed in section 5.

2. THE MAGNETIC SWITCH FOR NORMAL COMPACT OBJECTS AND NON-ROTATING BLACK HOLES

2.1. The Classical Magnetic Switch

In the original magnetic switch model presented in MEGPL, the flow behavior depends on the ratio of the Alfvén velocity in the inner disk corona $V_{A0} \equiv B_{p0}/(4\pi\rho_{c0})^{1/2}$ to the escape velocity there $V_{esc0} = (2GM/R_0)^{1/2}$, where B_{p0} is the strength of the poloidal magnetic field protruding from the disk into the corona at radius R_0 , ρ_{c0} is the density of the corona there, M is the mass of the black hole, and G is the gravitational constant. When $\nu \equiv V_{A0}/V_{esc0} < 1$, gravity dominates magnetic forces (the plasma is bound initially) and the character of the flow is similar to a Parker wind (with collimation): azimuthal magnetic field coiled in the corona uncoils upward to slowly accelerate the flow through a series of critical points. Depending on the parameters, the resulting jet speed is approximately equal to the escape speed at the base of the outflow (Kudoh & Shibata 1996), which is somewhat interior to the last stable orbit in the relativistic Schwarzschild black hole case (Koide et al. 1998a). When $\nu > 1$, magnetic forces dominate gravity and, for sufficiently high ν , render the latter negligible. (The coronal plasma is unbound.) As in pulsar wind theory, the outflow velocity then is determined not by gravitational effects, but by the magnetization parameter

$$\sigma_0 \equiv V_{A0}^2 R_0^2 / (4V_{i0} c R_L^2) \quad (1)$$

which is a measure of the amount of work done on the injected plasma; here, V_{i0} is the velocity with which matter is injected, $R_L \equiv c/\Omega$ is the radius of the light cylinder, and Ω is the angular velocity of the poloidal magnetic field at R_0 . For relativistic flows, $\gamma_j \approx \sigma_0$ appears to be a good approximation for the final MHD wind/jet velocity (Camenzind 1989; Henriksen 1989).

A transition between the two types of outflow then is induced by increasing the magnetic field strength B_{p0} until $\nu > 1$, whereupon significantly higher jet speeds occur. This magnetic switch has several properties that make it an attractive model for the difference in morphology between class I and class II extragalactic radio sources (Fanaroff & Riley 1974): 1) the transition is sharp, occurring with increasing jet power; 2) jets produced when $\nu < 1$ are transonic, while those for $\nu > 1$ are highly supersonic, and 3) even statistical behavior observed in large samples of radio galaxies of different power and optical magnitude is reproduced (see Meier et al. 1997b and Section 4.1 below).

2.2. Failure of a Change in Magnetic Field Strength to Explain the FR I/II Break

However, as presented in MEGPL, the original magnetic switch, triggered by either increasing the coronal magnetic field or decreasing the coronal density, fails to explain the FR I/II break, chiefly because it fails to explain why radio sources appear to maintain their FR morphology for long periods of time — at least as long as the flow time from galactic center to lobe (10^{6-7} yr). There is no reason to expect the strength of the magnetic field threading disk and hole (or the coronal density) to remain fixed at

high or at low values over such long time scales. Indeed, one expects that these quantities will be distributed fairly equally about a mean, and on average will be the same for galaxies of the same mass. The argument is as follows. The structure of an accretion disk is a function of the black hole mass $m_9 \equiv M / 10^9 M_\odot$, the accretion rate \dot{M} , the viscosity parameter α , and position in the disk scaled to the Schwarzschild radius (Shakura & Sunyaev 1973; Novikov & Thorne 1973). Now, there is growing evidence that the black hole mass, even in presently inactive objects, is approximately proportional to the mass of the central spheroidal bulge of stars (see, *e.g.*, Kormendy & Richstone 1995) such that

$$\log m_9 \approx -0.5M_B - 10.5 \quad (2)$$

where M_B is the absolute blue optical magnitude of the bulge. In addition, while the instantaneous accretion rate will vary dramatically on short time scales (years), because the hole is fed by galactic stars and gas, over the very long term the average accretion rate also should be roughly proportional to the bulge mass (a perhaps necessary condition for equation [2] to be valid). Therefore, to first order, we expect the average accretion rate

$$\langle \dot{m} \rangle \equiv \langle \dot{M} \rangle / \dot{M}_{Edd} = \langle \dot{M} \rangle / (1.4 \times 10^{26} \text{ g s}^{-1} m_9) \quad (3)$$

to be a constant, proportional to the average amount of matter shed per unit time into the nucleus and onto the hole by a galactic bulge of a given optical magnitude, divided by the mass of the black hole in that nucleus. (Note that the definition of \dot{m} here does not include an efficiency of conversion of accreting matter into radiation, allowing for maximum values somewhat greater than unity [$\dot{m}_{Edd} = 2.5 - 10$], depending on the spin of the black hole. It also assumes that the accretion is continuous; to take intermittent accretion into account, we will add a duty cycle parameter below.) Furthermore, detailed simulations of the magneto-rotational instability (Stone et al. 1996; Brandenburg et al. 1996) have shown that $\alpha \sim 10^{-2}$ is a fairly good approximation for turbulent accretion flows, presumably independent of black hole mass to first order. And, finally, jets are believed to be ejected from near the black hole horizon (*i.e.*, from just inside the last stable orbit, Koide et al. 1998a), rendering the position parameter R_0/R_{Sch} a near-constant value for all objects. Therefore, ignoring external influences, *over periods of time comparable to the flow time from nucleus to lobe, all parameters that affect the disk structure equations are expected to be, at most, functions of the black hole/galactic bulge mass only.* On average, one expects bulges of the same mass to produce the same type of accretion disk in the nucleus, with similar magnetic field and coronal density, and, therefore, the same type of jet (either all slow or all fast). It is not expected that there will be a spectrum of jet structures that maintain themselves for millions of years. Yet the observations show that just such a range of radio powers and morphologies exists, and that a radio source remains an FR I or II for longer than a flow time.

3. THE MAGNETIC SWITCH IN THE ROTATING BLACK HOLE ENVIRONMENT

In order to lift the degeneracy in expected jet speeds and morphologies, we shall take as an additional param-

eter the rotation rate of the magnetic field, as determined by the black hole rotation rate itself. This section develops the model of the accreting rotating black hole system, the production of radio jets, and the triggering of the magnetic switch.

In order to compute observable quantities, we must assume an accretion scenario in the black hole system. For definiteness, we choose a rather benign (standard) accretion disk in which electron scattering dominates free-free absorption and gas pressure dominates radiation pressure, and we scale the results to a rather low accretion rate ($\dot{m} \sim 10^{-3}$). While the details will change depending on the exact accretion model and rate, the basic conclusions herein will not, even in the extreme cases of near-Eddington accretion (radiation pressure dominated) or very low, advection-dominated accretion flow (ADAF; Narayan & Yi 1995).

3.1. The Generalized Magnetic Switch

The first task is to generalize the magnetic switch theory to include rotation as a triggering parameter, in addition to magnetic field strength and plasma density. Consider a general magnetic rotator of size R_0 , poloidal magnetic field B_{p0} , and angular velocity Ω . Following Blandford & Payne (1982), the work done on the plasma trapped in the field lines, resulting in an outflowing magnetohydrodynamic (MHD) wind or jet, is

$$L_{MHD} = B_{p0}^2 R_0^3 \Omega / 2 \quad (4)$$

for non-relativistic flow. Now, for a normal Parker-type wind, the plasma in the injection region is in hydrostatic equilibrium, with only a slight force imbalance outward that slowly accelerates the outflow through a critical point until it reaches escape velocity and leaves the system (see, *e.g.*, Meier 1982). This is also true of MHD winds, although the critical point structure and geometry are more complex. However, based on the magnetic switch mechanism described by MEGPL, there should exist a critical power, given by the liberation of an escape energy in a free-fall time

$$L_{crit} = E_{esc0} / \tau_{ff0} = 4\pi \rho_{c0} R_0^2 \left(\frac{GM}{R_0} \right)^{3/2} \quad (5)$$

such that if L_{MHD} exceeds L_{crit} , then the plasma becomes unbound — even in the injection region itself. That is, the outward magnetic and centrifugal forces there strongly exceed gravity, accelerating the plasma to greater than the escape velocity within R_0 and eventually to a much greater final velocity. *The magnetic switch luminosity, then, plays the same role in MHD acceleration as the Eddington luminosity plays in radiative acceleration.* For Keplerian disks (with $\Omega = \Omega_K \equiv (GM/R_0)^{3/2}$), the condition $L_{MHD} > L_{crit}$ reduces to the original magnetic switch condition $V_{A0} > V_{esc0}$. However, for a non-Keplerian rotator of *fixed* magnetic field strength and plasma density, there should exist a critical angular velocity

$$\Omega_{crit} = \Omega_K \frac{V_{esc0}^2}{V_{A0}^2} \quad (6)$$

such that if Ω exceeds Ω_{crit} , then the magnetic switch also should be triggered and a fast jet of the type found by MEGPL should ensue.

The author tested this hypothesis by performing numerical MHD simulations similar to MEGPL, but holding B_{p0} fixed and varying the disk rotation speed instead. The left panel of Figure 1 shows the resulting jet speed as a function of Ω . For angular velocities below Ω_{crit} the terminal jet/wind speed is approximately the escape speed at the injection point. When $\Omega > \Omega_{crit}$, the material is unbound and quickly accelerated (in a well-collimated jet, similar to MEGPL) to a speed such that a large fraction of the power L_{MHD} is in the form of kinetic energy (see the right panel of Figure 1). It is this strong difference in the character of the outflows below and above Ω_{crit} that is so similar to the FR I/II division: while the total power varies smoothly as L_{MHD} exceeds L_{crit} , the character of the outflow varies dramatically from a transonic, magnetic-energy-dominated jet to a highly supersonic, kinetic-energy-dominated one.

The details of the behavior of the curves in Figure 1 can be understood qualitatively as follows. When $\Omega < \Omega_K$, the injected plasma is no longer supported fully by rotation. Therefore, as soon as it emerges from the disk boundary, it dynamically contracts in cylindrical radius, seeking a new Keplerian equilibrium. The jet then is ejected from this new, smaller, radius R'_0 with a speed similar to the Keplerian velocity there and a power slightly *larger* than that given by equation (4), because of compressional increase in the axial magnetic field component ($B'_{z0} \propto R'_0{}^{-2}$). If Ω is decreased further, the plasma contracts more, increasing the eventual jet velocity slightly. On the other hand, when $\Omega > \Omega_K$, the reverse occurs, with the plasma expanding to a new injection radius. As Ω increases, the value of Ω_{crit} calculated from equation (6) changes as well, chiefly because only the radial component of the magnetic field is important in the expanded state ($B'_{R0} \propto R'_0{}^{-1}$). This increases the critical value to $\Omega'_{crit} = \Omega'_K V'_{esc}{}^2 / V'_{AR}{}^2$ (where V'_{AR} is the *radial* component of the Alfvén velocity at the new injection radius), which is greater than the value in equation (6). Finally, well above the magnetic switch (when $\Omega \gg \Omega_{crit}$) the well-collimated jet flow gives way to a less-collimated radial wind, and the increase in outflow speed with rotation speed begins to break down. It is not clear whether such a decrease at high Ω will occur in the relativistic case, where light cylinder effects will be important. Relativistic MHD simulations are needed to investigate this behavior.

Some brief comments should be made about boundary conditions. In these simulations, the kinematic and magnetic properties of the inflowing matter at the equator (the “disk corona”) are fixed throughout the calculation. However, some authors allow these parameters to be determined by the solution, particularly the azimuthal and radial components of the field at the equator and the inflow velocity there (see, *e.g.*, Ustyugova et al. 1999). Both of these sets of conditions (fixed or self-adjusting) are easy to apply numerically, and each is appropriate under different circumstances. The latter is useful for generating steady state solutions to compare with Blandford & Payne (1982)’s self-similar, semi-analytic models. In this case, conditions at the base of the outflow re-adjust themselves,

subject only to the strength of the vertical magnetic field, the density of inflow, and the speed and shear of the disk rotation. The system finally reaches a steady state with parameters lying on (or near) the Blandford-Payne solution surface in $(\kappa, \lambda, \xi'_0)$ -space (see BP), with the flow varying smoothly from the outer regions all the way back to the equatorial boundary.

On the other hand, fixing the inflow conditions on the equator, as we have done here, is perhaps more appropriate for studying the astrophysical situation where the magnetic field is anchored in an accretion disk (or other type of rotator). In that case the local magnetic field is determined by processes internal to the rotator, not by the outflow that originates above it. When the boundary conditions are fixed, a steady flow still develops above the disk, and the azimuthal and radial fields and flow velocity in the corona also re-adjust. However, because that resulting outflow does not necessarily match onto the fixed disk boundary conditions, there is a transition region between the disk and the base of the outflow region, in which the magnetic field and velocity dramatically change in magnitude and direction. It is not yet fully clear whether this transition region merely provides a way to connect an outflow solution that would have occurred anyway to the disk conditions, or whether it plays an active role in determining what outflow solution is chosen. What is clear is that the values of the parameters chosen on the disk *below* the transition region *do* matter: the flow changes dramatically with the strength of the poloidal *and* azimuthal field specified and, to a lesser extent, with the angle of the poloidal field (Meier, Payne, & Lind 1996; MEGPL). Furthermore, jet simulations in which a substantial *equatorial* field (azimuthal plus radial) is specified seem to display more collimation, presumably because of the strong azimuthal field that is initially present or that develops after a few turns of the disk.

3.2. The Rotating Black Hole Model of Jet Production

The proposed model of jet production from the accreting, rotating black hole system is essentially a marriage between the disk acceleration model of Blandford & Payne (1982) and the rotating black hole acceleration model of Blandford & Znajek (1977) and MacDonald & Thorne (1982). The former authors considered the case when the magnetic field threads only the Keplerian portion of the disk, while the latter examined the situation when it threads both hole and disk. In this paper we consider the intermediate case when the magnetic field threads both a region of the system outside the static limit that does not experience appreciable frame dragging and a region closer to the black hole that does — the ergosphere. The main features of this model are the following: (1) Unlike the BZ model, the magnetic field does not have to thread the horizon itself in order to extract the black hole rotational energy, which avoids the problems discussed by Punsly & Coroniti (1990a), and the primary source of material in the jet can be a corona created by the accretion disk itself, not necessarily particles created in spark gaps near the horizon. (2) It is unlike the BP model because the disk and field there are frame-dragged by the hole relative to an observer at infinity, and thus the jet production couples well to the black hole spin, extracting rotational energy even though it is disk rotation that accelerates the

jet.

This model is very similar to that of PC, who studied steady state winds from the ergospheric region of a rotating hole. We note here an additional feature of such a system that occurs when time dependence is taken into account: as shown in the Appendix, when a plasma with an appreciable poloidal magnetic field is present in the ergospheric region, the differential dragging of frames will increase the azimuthal magnetic field at the expense of the hole's rotational energy. If, as a result of dynamo action, this also is accompanied by a corresponding increase in the poloidal component, this will have the effect of increasing the jet power produced near a rotating black hole to a value substantially larger than that for a disk around a Schwarzschild hole.

3.2.1. MHD output power

When a black hole is spinning rapidly, the accretion disk can extend well into the ergosphere — the region where local observers must rotate with the hole — with equatorial radius $R_e = 2GM/c^2$. For a nearly-maximal Kerr hole ($j \rightarrow 1$), the last stable orbit reaches into this region — very close to the horizon at $R_H = (1 + \sqrt{1 - j^2}) GM/c^2$, where $j \equiv J/(GM^2/c)$ is the normalized angular momentum of the hole (equal to “ a/M ” in geometric units). Now, consider a loop of coronal magnetic field B_{p0} with one foot anchored in the ergosphere and one outside.¹ Recently Hayashi, Shibata, & Matsumoto (1996) and Romanova et al. (1998) have shown that even in a Keplerian flow, differential rotation in the inner disk can modify closed coronal loops, stretching and twisting them into long, virtually-open vertical helical structures of the type needed to accelerate MHD winds and jets. If the differential rotation is further augmented by frame dragging, then the work done on the field and outflow derives its power not only from the Keplerian rotation of the disk, but also from the rotation of the ergosphere itself relative to the point where the outer foot is anchored (see the Appendix). The system then appears to an observer at infinity as a simple magnetic rotator with size $R_0 = R_e$, magnetic field B_{p0} , and angular velocity $\Omega \geq \Omega_e \approx 0.4\Omega_H \approx 0.4j/(2GM/c^3)$, where Ω_e and Ω_H are the angular velocity of the ergosphere equator and hole, respectively. The form of equation (4) for a relativistic rotator² yields an MHD power for the accreting system of

$$L_{MHD} = B_{p0}^2 R_0^4 \Omega^2 / 4c \quad (7)$$

$$= 1.1 \times 10^{48} \text{ erg s}^{-1} \left(\frac{B_{p0}}{10^5 \text{ G}} \right)^2 m_9^2 j^2 \quad (8)$$

which is a comparable power to that of the BZ mechanism for the same poloidal field strength.

3.2.2. Disk magnetic field strength

Livio, Ogilvie, & Pringle (1999) have argued that the MHD power from the accretion disk (the BP process, given

¹This distinction is somewhat arbitrary, as frame dragging takes place outside the ergosphere as well, although at an increasingly smaller rate as one moves away from the hole, and it also increases within the ergosphere as one moves toward the horizon. The important point to note is that a field loop with its feet at different disk radii will receive a twist similar to that in a normal Keplerian disk, but driven by the differential dragging of frames in addition to any shearing fluid flow within the ergosphere.

²Equation (7) also can be derived from equation (1) and the relations $\gamma_j = \sigma_0$ and $L_{MHD} = L_j \approx \gamma_j \dot{M}_j c^2$, where $\dot{M}_j = 4\pi R_0^2 \rho_{c0} V_{i0}$ is the mass lost in the jet.

by equation [4]) and that from the black hole (the BZ process, given by equation [7] with $\Omega = \Omega_H$) are, at best, comparable, and, at worst, entirely dominated by the former if the hole spin is small. They, therefore, conclude that the BZ process will never be important and that the spin of the black hole is probably irrelevant for the expected electromagnetic power of the system. This author agrees with the basic tenets of Livio, Ogilvie, & Pringle (1999) that the disk and hole power will be comparable, but not with their ultimate conclusion on the unimportance of the spin. The key difference is that, in the ergosphere, the MHD power of the disk itself (equation 8) should depend on the spin of the black hole. In addition, when the hole is rotating, a much larger poloidal magnetic field strength is allowed than estimated by these authors, yielding black hole rotation-driven powers comparable to those observed in extragalactic radio sources.

First, consider the non-rotating Schwarzschild black hole case. The disk will be a standard Keplerian one, with internal disk field given by (Shakura & Sunyaev 1973)

$$\frac{B_{d0}^2}{8\pi} \approx \alpha p_{d0} \quad (9)$$

where p_{d0} is the local internal disk pressure. Now the source of a coronal loop of field B_{p0} will be this (largely azimuthal) disk field, first protruding into the corona and then growing as the loop is sheared and expanded upward. However, in a thin Keplerian disk, if the poloidal field is allowed to grow to the same order as B_{d0} , then the expected MHD power from equation (4) would be orders of magnitude greater than the accretion luminosity

$$\begin{aligned} \frac{L_{MHD}(B_{p0} = B_{d0})}{L_{acc}} &= \frac{\alpha c_{s0}}{|V_{R0}|} \\ &= 3.8 \times 10^3 (\alpha_{-2} m_9)^{1/10} \dot{m}_{-3}^{-1/5} \quad (10) \end{aligned}$$

where c_{s0} is the sound speed in the disk, V_{R0} is the inward accretion drift speed, and the notation α_{-2} represents $\alpha/10^{-2}$. (As discussed earlier, we have used a gas-pressure, electron-scattering-dominated disk, but the results are similar for other types of disks.) There is not enough accretion luminosity to support this MHD power by factors of several thousand. As B_{p0} grows to a even a small fraction of B_{d0} , the MHD disk power becomes a substantial fraction of L_{acc} . At that point, a significant amount of angular momentum is removed from the disk by the outflow, altering the disk structure and enhancing the local accretion rate. In order that the accretion draining the inner disk remain in a steady state with that feeding it from the outer disk (and not, for example, launch into a series of bursts that each destroy the inner disk entirely), B_{p0} must be self-limited to about the value postulated by Livio, Ogilvie, & Pringle (1999), or $B_{p0} \approx B_{d0} (H_0/R_0) \ll B_{d0}$, where H_0 is the half-thickness of the disk at R_0 .

However, when the central object is a rotating black hole, the situation will be quite different. As before, when B_{p0} grows to a fraction of B_{d0} , a significant MHD outflow will develop, exerting a braking torque on the inner portion of the disk. Because of the differential frame dragging, however, even if *all* the Keplerian angular momentum were removed by the outflowing MHD power, the disk material still will be sheared *by the metric itself*, continuing to increase the local magnetic field strength and continuing to produce MHD power. The Appendix shows quantitatively how this occurs in the Kerr metric, producing field enhancement everywhere in the ergospheric region. Tension in this growing, working field then produces a back-reaction on the disk plasma falling toward the hole, accelerating it relative to the rotating frame in a direction *retrograde* to the black hole spin. By the time the magnetized accretion flow enters the black hole, it could have a significant *negative* angular momentum which, when added to the hole, would decrease the spin. Therefore, because of frame dragging, power flows from hole to disk to field and finally to the outflow, exerting a braking torque on the hole itself. No longer self-regulated by the accretion flow, B_{p0} in the ergospheric region above the disk now can continue to grow at the expense of the hole rotational energy to order B_{d0} , given by the disk solutions with a Kerr metric (Novikov & Thorne 1973). For the gas pressure/electron-scattering accretion model assumed here, this value is

$$B_{p0} \approx B_{d0} = 3.4 \times 10^4 \text{ G } \alpha_{-2}^{1/20} m_9^{-9/20} \dot{m}_{-3}^{2/5} \quad (11)$$

Equation (8) then becomes

$$L_{MHD} = 1.3 \times 10^{47} \text{ erg s}^{-1} \alpha_{-2}^{1/10} m_9^{11/10} \dot{m}_{-3}^{4/5} j^2 \quad (12)$$

(This differs from equation (16) of Moderski & Sikora 1996 by a factor of α , from equation (9), and a factor of $\sim 0.4^2$ from the slightly smaller ergospheric rotation rate.) While L_{MHD} appears to scale with m_9 and \dot{m} in a manner similar to an accretion luminosity, it is important to note that it does so only because of the scaling on B_{d0} . The energy liberated is derived mainly from the rotation of the hole itself and potentially much larger than the accretion luminosity ($L_{acc} \approx 10^{43} \text{ erg s}^{-1} m_9 \dot{m}_{-3}$).

3.2.3. Observed radio power

To turn L_{MHD} into an observed radio power, we note that, over long periods of time, the central engine may generate a jet only a fraction ζ of the time. Furthermore, only a fraction ϵ of this average power is radiated at GHz frequencies in a 1 GHz bandwidth and observed with standard radio telescopes. From millimeter and optical observations of repeated outbursts of radio galaxies and quasars (see, *e.g.*, Robson 1992), we estimate typical duty cycle values to be $\zeta \sim 0.01 - 0.1$. The radio efficiency is also very uncertain, but we note that for the microquasars GRO J1655-40 and GRS 1915+105, estimates of ϵ are of order 10^{-5} or so, just for the instantaneous moving jet (Meier 1996). A canonical value of $\epsilon \sim 10^{-3}$ was chosen for these calculations by comparing equation (12) with the maximum observed radio source power ($10^{27} \text{ W Hz}^{-1}$) for

a radio galaxy that should have a $10^9 M_\odot$ hole in its nucleus ($M_B \approx -21.0$). This value for ϵ is consistent with total conversion rates of $\sim 0.01 - 0.1$ (see, *e.g.*, Leahy 1991), with only a fraction of that radiated in a 1 GHz bandwidth. Scaling to these values, the calculated radio power for different black hole spins is

$$P_{rad} = \epsilon \zeta L_{MHD} / 10^9 \text{ Hz} \quad (13)$$

$$= 1.3 \times 10^{27} \text{ W Hz}^{-1} m_9^{11/10} j^2 \times \left(\epsilon_{-3} \zeta_{-1} \alpha_{-2}^{1/10} \dot{m}_{-3}^{4/5} \right) \quad (14)$$

where \dot{m} is still the average *outburst* accretion rate only, not that averaged over the entire duty cycle.

3.3. The Magnetic Switch as the FR I/II Break

The final step in the model is to identify the magnetic switch as the cause of the FR I/II break. That is, one should observe a distinct change in the character of the jet produced when $L_{MHD} = L_{crit}$, or when the radio power attains the critical value

$$P_{rad,mod}^{FR} = \epsilon \zeta L_{crit} / 10^9 \text{ Hz} \quad (15)$$

To compute an observed break power we need an expression for the corona density ρ_{c0} at R_0 . Of course, coronal physics is poorly understood, even for the sun. Nevertheless, we can obtain a rough estimate by assuming that the corona is produced locally by the accretion disk, so the disk and corona densities should scale together as³

$$\rho_{c0} \approx \eta \rho_{d0} \quad (16)$$

where ρ_{d0} is the internal disk density at R_0 and $\eta \ll 1$ is a parameter which, while not necessarily a true constant, is assumed to vary sufficiently slowly with the other parameters that it does not affect significantly the scaling of our results with m_9 , j , and \dot{m} . The parameter η is expected to be quite small; in the solar corona, for example, $\eta_\odot \equiv \rho_{c\odot}/\rho_\odot(\tau=1) \sim 10^{-8} - 10^{-11}$ in the region between the photosphere and $2R_\odot$. If the corona is a pair plasma, η (which is a mass ratio) could be very small indeed. Combining equations (5), (15), and (16), and again using the gas pressure/electron-scattering disk, one obtains

$$P_{rad,mod}^{FR} = 4.8 \times 10^{25} \text{ W Hz}^{-1} m_9^{13/10} \times \left(\epsilon_{-3} \zeta_{-1} \alpha_{-2}^{-7/10} \dot{m}_{-3}^{2/5} \eta_{-11} \right) \quad (17)$$

This is the magnetic switch model prediction for the locus of the FR I/II break as a function of black hole mass.

4. APPLICATIONS AND DISCUSSION

This section applies the model to the FR I/II break in the radio-optical plane, shows that the rotationally-triggered magnetic switch *is* consistent with long source morphology lifetimes, and addresses the more general questions of evolution and radio loud *vs.* radio quiet sources. The important features of the model and its applications are shown in figure 2.

³Another possible scaling would be with both ρ_{d0} and the internal disk temperature T_{d0} (*i.e.*, with p_{d0}). This yields a slightly weaker M_R slope (-0.55) in equation (19) below, but still within the observational errors.

4.1. The “OLWL” Relation in the Radio-Optical Plane

Owen & Laing (1989), Owen & White (1991), and Ledlow & Owen (1996) have shown that FR I and FR II type radio galaxies occupy different regions of the $\log P_{rad,obs} - M_{R,24.5}$ plane, where $\log P_{rad,obs}$ is the observed radio power at 1400 MHz (in W Hz^{-1}) and $M_{R,24.5}$ is the galaxy optical red magnitude measured to a surface brightness of 24.5 magnitudes per square arcsecond. In particular, the tendency for a galaxy of a given magnitude to transition from an FR I to an FR II appears to be a strong function of optical magnitude. The dividing line is given approximately by

$$\log P_{rad,obs}^{FR} = -0.66 M_{R,24.5} + 10.35 \quad (18)$$

or $P_{rad,obs}^{FR} \propto L_{opt}^{1.65}$. The error in the coefficient of $M_{R,24.5}$ is at least ± 0.1 and in the intercept at least $\pm 0.3 - 0.5$. The Owen-Laing-White-Ledlow (OLWL) relation is a more precise statement of the Fanaroff & Riley class division, so care must be taken when classifying radio galaxies based on their radio power only. There exist FR II radio galaxies with quite small powers (occurring in less bright elliptical galaxies), as well as FR I objects with very high radio power (occurring in very bright galaxies).

From the magnetic switch model for the FR I/II break, it is possible to calculate a theoretical relation for the observed break power to compare with equation (18). Using equation (17) to define the break, equation (2) to convert black hole mass to galaxy bulge blue optical magnitude, and a standard $B - R \sim 1.5$ to convert to elliptical galaxy blue magnitudes to red, one obtains

$$\begin{aligned} \log P_{rad,mod}^{FR} &= -0.65 M_R + 11.1 \\ &+ \log(\epsilon_{-3} \zeta_{-1} \alpha_{-2}^{-7/10} \dot{m}_{-3}^{2/5} \eta_{-11}) \quad (19) \end{aligned}$$

Given the uncertainties in the observed slope, in the scaling of the coronal density, and in the parameters ϵ , ζ , and, especially, η , the good numerical agreement between equations (18) and (19) is rather fortuitous, of course. The important points to note are as follows:

- The basic trend that brighter galaxies, with their more massive black holes, should undergo the magnetic switch at a higher jet power is a general feature of the model (see figure 2). The ultimate source of this trend is that the critical jet power is proportional to the size of the ergosphere squared times the disk coronal density there. If this density were uniform for all black holes, it would produce a trend slightly steeper than $P_{rad}^{FR} \propto L_{opt}^2$, because the galaxy M/L ratio increases with galaxy L_{opt} (Faber et al 1987); however, as densities tend to decrease as the size of the accreting system increases, the trend should be *less* steep than this.
- Although the uncertainties are great, the intercept is consistent with the values of the parameters chosen here, in particular with the very low value of η . That is, *the observations are entirely consistent with the jet material originating in the coronae of the black hole accretion disks*, and grossly inconsistent — by more than ten orders of magnitude — with the jet ejecting a large fraction of the accretion disk itself.

Incidentally, the present model is *not* inconsistent with observations that FR I jets may decelerate on kiloparsec scales (Laing 1996). Indeed, it suggests a reason for such deceleration to occur more readily in FR I sources. Jets with $L_{MHD} < L_{crit}$ are transonic in the simulations here and in MEGPL. Such jets are more prone to deceleration than highly supersonic flows (Bicknell 1985). Note that deceleration of relativistic parsec-scale jets to nonrelativistic flow on kiloparsec scales is needed in *any* model, magnetically switched or not, to explain head-tail and wide-angle-tail sources in clusters, whose jets are bent by motion of only a few thousand kms^{-1} through the intracluster medium.

4.2. Black Hole Spindown and the Early Evolution of FR II Radio Sources

Because the black hole spin is the assumed source of power, there should be a critical spin j_{crit} — corresponding to a critical hole angular velocity $\Omega_{H,crit}$ — such that the magnetic switch is triggered when the hole is spun up to this value. Equating $P_{rad,mod}^{FR}$ and $P_{rad,mod}$ (or L_{MHD} and L_{crit}) one obtains

$$j_{crit} = 0.20 \alpha_{-2}^{-2/5} m_9^{1/10} \dot{m}_{-3}^{-1/5} \eta_{-11}^{1/2} \quad (20)$$

Now, while this relation is a very weak function of m_9 and \dot{m} , and α is considered to be known to within a factor of ten or better, the exact value of j_{crit} is still very uncertain because of the parameter η . Indeed, a large value (dense corona) would make $j_{crit} > 1$, implying that even a maximal Kerr hole would not trigger the switch. Below observational tests are proposed to confirm the low choice of η in this paper.

Note that, independent of the magnetic switch model, if the source of the radio jet power is, indeed, the black hole rotational energy, then simple arguments show that at the FR I/II transition, j must be of order 0.1 in any case. From the OLWL results and the bivariate radio luminosity function itself, it appears that, for a galaxy of a given mass, the maximum possible radio power is about 100 times the power at the FR break. Therefore, for any model where $P_{rad} \propto j^2$, we find that

$$j_{obs}^{FR} \approx \left(\frac{P_{rad}^{FR}}{P_{rad}^{max}} \right)^{1/2} \sim 0.1 \quad (21)$$

The magnetically-switched, rotating black hole model further predicts that FR II sources contain the seeds of their own destruction. The jet extracts rotational energy from the black hole until $j < j_{crit}$, whereupon the jet transitions to an FR I source. Now, in the absence of external effects, the spindown rate is proportional to j^2 , and therefore the hole rotational energy

$$\begin{aligned} E_{rot} &= M c^2 \left[(1 + j^2/4)^{1/2} - 1 \right] \\ &\approx 1.6 \times 10^{62} \text{ erg } m_9 j^2 \quad , \quad (22) \end{aligned}$$

rendering the spindown an exponential process, with a time scale

$$\begin{aligned} \tau_{spindown} &= \frac{E_{rot}}{\zeta L_{MHD}} \\ &= 4.1 \times 10^8 \text{ yr } \alpha_{-2}^{-1/10} m_9^{-1/10} \dot{m}_{-3}^{-4/5} \zeta_{-1}^{-1} \quad (23) \end{aligned}$$

where ζ is the duty cycle parameter defined earlier. This spindown time is $\lesssim 10^9$ yr time scale found for the cosmic evolution of powerful extragalactic radio sources (Schmidt 1972; Wall & Jackson 1997). A plausible scenario, then, is that a fraction of black holes are born with very high spin (FR II sources) and subsequently experience a strong density evolution, disappearing after $\tau_{spindown}$ or so. Note that the local FR I space density exceeds that of FR II sources at all epochs, so that expired FR II sources could easily be hiding in the FR I population (Jackson & Wall 1999; Jackson, private communication).

Note also that, like the accretion time

$$\tau_{acc} \equiv M / \dot{M} = 4.5 \times 10^{12} \text{yr} \dot{m}_{-3}^{-1} \zeta_{-1}^{-1} \quad (24)$$

$\tau_{spindown}$ is virtually independent of black hole mass (although much shorter). Therefore, in the absence of other effects, even *stellar* mass black holes like GRO J1655-40 or GRS 1915+105 are expected to retain their spin over $\sim 10^9$ yr as they use their rotational energy to drive radio jets. Such a long spin lifetime should have implications for models for galactic microquasars.

During the entire lifetime of the radio source, an energy comparable to E_{rot} should be liberated into the lobes. That is, extended radio sources are the remnants of formerly rapidly-rotating black holes. This amount of energy is consistent with, and in fact somewhat larger than, the total energy content of extended radio sources in relativistic particles and magnetic fields (DeYoung 1976). This allows for a significant fraction of this energy to have been converted to other forms (*e.g.*, heating of the intergalactic medium) or radiated away.

4.3. Little Evolution for FR I (and FR II) Sources at Late Times?

The fact that E_{rot} is proportional to j^2 , and not to just j , for example, means that the spindown time is the same no matter how rapidly or slowly the hole is rotating. The model predicts therefore, that after turning into an FR I source, the object will continue to display pure luminosity evolution on a $\tau_{spindown}$ time scale. However, recent analyses of the radio source counts and redshift data (Urry & Padovani 1995; Wall & Jackson 1997) conclude that the FR I population evolves little or not at all. Modeling this sort of behavior is very difficult, especially in a universe where everything involved with AGN seems to evolve on at least a cosmological time scale (galaxy formation and mergers; the rate of stellar death [which may feed gas into the nucleus]; even radio quiet quasars; *etc.*). Below are some ideas for halting, or at least slowing, the evolution of FR I sources in this model; however, much more work needs to be done on this problem:

- *Constant low-powered jet from outside the ergosphere.* After spinning down, the black hole loses most of its ergosphere and its ability to create a large poloidal field strength in the disk. The field strength is expected to drop to the value suggested by Livio, Ogilvie, & Pringle (1999), yielding an expected jet power of

$$L_{MHD}^{min} = 9 \times 10^{40} \text{erg s}^{-1} \alpha_{-2}^{-1/10} m_9^{9/10} \dot{m}_{-3}^{6/5} \quad (25)$$

⁴Of course, as discussed earlier, due to a lack of a consistent long-term jet direction, this power may never manifest itself as an extended radio source. Here it will be assumed that it does; if not, the conclusions will be stronger.

which, with efficiency factors similar to those used above, could generate radio emission of up to $\sim 10^{21}$ W Hz⁻¹. A radio source of this power is not expected to evolve much, unless \dot{m} evolves. However, this is a very weak power — much smaller than many FR I radio galaxies, which also presumably do not evolve much. Furthermore, if the accretion events have rather random angular momenta, then this minimum jet has no preferred direction. It is likely to point in random directions with each event, never developing into an extended source, and perhaps appearing radio quiet.

- *Periodic spinup of the black hole.* On the other hand, if the short-term accretion events have systematically the same angular momentum direction, as might be the case for a galaxy collision or merger, then while they would keep the above weak jet oriented in the same direction, they also would tend to re-orient and spin up the hole (Wilson & Colbert 1995; Natarajan & Pringle 1998). This, or the direct merger of two black holes, would re-ignite the ergospheric jet. Then, if the galaxy merger rate evolved on a very long time scale (say, $\gtrsim 5 \times 10^9$ yr), the shorter time scale spindown process would become slave to the spinup process, with the average radio power being a function of the rate at which angular momentum is accreted onto the hole. At low redshifts, then, both FR I and the occasional re-kindled FR II objects would evolve on the longer merger evolution time, not $\tau_{spindown}$.

4.4. Radio Loud vs. Radio Quiet?

The model proposed here deals mainly with the difference between two radio loud populations — the FR I and II sources. However, it also has implications for the difference between radio loud and quiet quasars as well. In particular, it suggests that radio quiet objects should be identified with very slowly-rotating, nearly-Schwarzschild black holes. At first, the minimum jet power (equation 25) appears to be a problem with this suggestion, as it predicts that all active galaxies should produce some sort of extended radio emission.⁴ However, even if an AGN does produce an extended radio source power of

$$P_{rad}^{min} \leq 9 \times 10^{20} \text{W Hz}^{-1} m_9^{9/10} \times \left(\epsilon_{-3} \zeta_{-1} \alpha_{-2}^{-1/10} \dot{m}_{-3}^{6/5} \right) \quad (26)$$

the apparent flux would be quite small: less than a few μ Jy for Seyfert galaxies at $z > 0.03$ and quasi-stellar objects at $z > 1$, and a few millijanskies total for nearby spiral galaxies. This amount of extended emission in spirals could be hidden easily by emission from supernova remnants, *etc.* Therefore, there should be a minimum spin rate j_{min} for the hole such that when $j < j_{min}$, it will appear radio quiet. While detailed simulations of jet production from rotating black holes, plus observational selection factors, need to be taken into account to determine a precise value

of j_{min} , we can estimate it here by equating the MHD power generated by the ergospheric and Keplerian disk jets (equations 12 and 25) and solving:

$$j_{min} = 0.83 \times 10^{-3} \alpha_{-2}^{-1/10} m_9^{-1/10} \dot{m}_{-3}^{1/5} \quad (27)$$

For spins slower than this, the wind/jet from the Keplerian portion of the disk outside the ergosphere will dominate the output MHD power.

Even if the minimum jet power turns out not to be a problem, one still needs to explain — quantitatively as well as qualitatively — why the radio power distribution is bimodal: radio quiet objects appear to be a separate class, not merely the fainter version of the powerful radio sources (Kellermann et al. 1989). One possible solution to this problem is the re-kindling the radio source through galaxy mergers or collisions. This is not a new idea (Wilson & Colbert 1995), but the model presented here, especially equation (23), gives a physical and quantitative basis for it. In the early universe, holes would have been born with a spectrum of rotational speeds. Those rotating rapidly would have produced extended radio sources, including holes in some (pre-)spiral galactic bulges, while those rotating slowly would have been radio quiet. All of these objects should have spun down in a few $\tau_{spindown}$ times and become radio quiet, according to the model. However, a subgroup — those in galaxies that experience repeated collisions and mergers — will be spun up again, at least partially to FR I class and very occasionally to FR II strength, re-kindling the radio source. This scenario is consistent with powerful radio sources appearing predominantly in elliptical galaxies, which now are believed to form from, or be strongly influenced by, mergers. An important corollary is that, early in their history, even the bulges of a significant fraction of spiral galaxies should have undergone a one-time extended radio source phase, lasting a few $\tau_{spindown}$ times and producing both FR I and II morphologies, but with considerably weaker luminosities than those associated with present-day giant elliptical radio sources.

The radio loud/quiet problem thus may be one of environment rather than being intrinsic to the system. However, before adopting such a simple model, it will be important to understand the strange case of the microquasar GRO J1655-40, which can be either radio loud or radio quiet during its X-ray outbursts (Tavani et al. 1996). It is not clear yet whether this is simply a short-term phenomenon or is fundamentally related to the macroquasar radio loud/quiet problem. So far, no model, including the one in this paper, appears able to explain completely this object's behavior.

4.5. Secondary Evolution in Accretion Rate and the Lack of FR I Quasars

It has been assumed in this paper that on a spindown time the average \dot{m} is fairly independent of black hole mass and remains at roughly $\sim 10^{-3}$. However, on a cosmological time scale this is not likely to be the case. Indeed, there is evidence (Wall & Jackson 1997; Jackson & Wall 1999) that some sources (class 'A') have a high accretion rate, indicated by strong, broad line emission, while others (class 'B') have a low (perhaps ADAF-like) rate. For the case where the latter objects are core-dominated and appearing as BL Lac objects, Wall & Jackson note that at least

some must have FR II sources as their parent population, not just FR I sources. One possible explanation of this is that the average \dot{m} may have been much higher in the early universe when the merger rate was high, and lower, perhaps even ADAF-like, now. Indeed, it appears that it is only the class 'A' objects that display rapid evolution (Jackson & Wall 1999). Then, present-day re-kindled FR I and II sources would both have a low average accretion rate, as well as a low evolution rate, and both have the potential for appearing as a BL Lac object if viewed end-on. Not all FR II sources seen this way would have to appear as quasars.

Ascribing a high accretion rate to class 'A' objects solves another puzzle concerning quasars — the fact that few, if any, radio loud quasars display FR I morphology. For $\dot{m} \sim 1$, equation (20) gives $j_{crit} \approx 0.05$, implying that even slowly-rotating black holes would produce an FR II morphology when the accretion rate is high. The right panel of figure 2 illustrates that the FR I portion of the quasar diagram is significantly smaller than that for radio galaxies; the exact size of the region depends critically on the definition of radio quietness.

5. TESTS OF THE MODEL

5.1. Observational Tests

This paper has shown that the magnetic switch mechanism, triggered by a rapidly spinning black hole, is consistent with a variety of observations concerning the FR I/II break. However, Bicknell (1995) has shown that an ISM model is consistent as well. In order to distinguish between these two, the following observational tests are proposed. The current model predicts the following:

1. The ensemble average of VLBI jet speeds for sources with FR I *morphology* should be distinctly slower than that for FR II sources. Until detailed general relativistic MHD simulations of very tenuous coronae in Kerr black hole ergospheres can be done (*cf.* Koide et al. 1998b), the exact values of the two mean velocities will be uncertain. The FR II mean should be highly relativistic (*i.e.*, $\gamma \sim 5 - 10$ or greater; see MEGPL). However, the FR I value may be more than mildly relativistic itself, as the escape velocity from the ergosphere is very close to c . Note the emphasis on FR morphology, rather than radio power. Radio power should *not* be used to distinguish between FR class in this test, unless it can be shown (using the OLWL relation) that the galaxy in question lies well within either the FR I or FR II region of the radio-optical diagram. Faint galaxies can have low-power radio sources that still have FR II morphology, and vice-versa.
2. Direct measurement of the accretion disk corona density in the ergosphere, using X-ray observations for example, should yield rather low mass densities ($\sim 10^{-15} \text{g cm}^{-3}$), perhaps either a $10^{12} \text{cm}^{-3} e^+e^-$ pair plasma or a very tenuous $10^9 \text{cm}^{-3} p^+e^-$ corona. These low values are needed for L_{crit} to be such that a radio power of $P_{rad,mod}^{FR} \sim 10^{25} \text{WHz}^{-1}$ is generated at the FR break. Significantly higher measured densities would render the corona too heavy for the magnetic switch to be triggered by any reasonable

jet power, and, in this model, always would predict slow jet velocities.

3. Recently, methods have been developed to estimate the spin of black holes by measuring the rotation rate of the innermost part of their accretion disks (Zhang et al. 1997; Sobczak et al. 1998). If such methods can be applied to extragalactic radio sources, one should find that the ensemble average of black hole spins for sources with FR I morphology should be distinctly lower than for those with FR II morphology.
4. There should exist a population of high-redshift, extended radio galaxies associated with the bulges of spiral or pre-spiral galaxies. They should include both FR I and II morphologies, but be weaker copies of the giant sources associated with ellipticals. The radio sources themselves should be readily detectable (for $m_9 = 10^{-2}$ and a redshift of 3, $P_{rad} \sim 10^{22-25} \text{ W Hz}^{-1}$ or $S \sim 4 - 4000 \mu\text{Jy}$), but their optical counterparts would be very faint if undergoing an initial burst of star formation ($M_R \sim 25$ for a $10^{10} M_\odot$ bulge at a similar redshift; Meier 1976) and even fainter ($M_R \sim 30$) if not. Preliminary estimates of their numbers are on the order of a few hundred to a few thousand per square degree — considerably smaller than the larger number of starburst galaxies at faint fluxes (Windhorst et al. 1995).

The first and third of these tests would provide support for the magnetic switch mechanism for the FR I/II transition. The second would support the choice for a small η . The third and fourth provide evidence for the proposal that the black hole spin is the switch triggering mechanism and the ultimate source of the radio power.

5.2. Numerical Tests

A number of numerical tests will be almost as important as the observational ones:

1. Firstly, as suggested by MEGPL, the magnetic switch needs to be confirmed by other groups performing numerical simulations, especially with a general relativistic MHD code, even if just for Schwarzschild black holes.
2. Secondly, general relativistic MHD simulations in Kerr geometry are needed to confirm that a substantial jet, whose power is directly related to the black hole spin, can be produced simply by threading the ergosphere with a magnetic field that is anchored further out. A simple vertical field should be sufficient initially, but simulations similar to those of Romanova et al. (1998), with closed coronal loops, would provide a more realistic test.
3. Finally, it will be important to reproduce in Kerr geometry the simple simulations performed in this paper, showing that increasing the black hole spin eventually triggers the magnetic switch. It also will be important to determine the speed, Mach number, and collimation properties of the outflow when the black hole spin is well above Ω_{crit} to see if the flow de-collimates (as it did in these non-relativistic simulations) or remains well-collimated.

6. CONCLUSIONS

The magnetically-switched, rotating black hole model for the FR I/II break is consistent with current black hole accretion models for active galactic nuclei, with MHD simulations of jet production, and with relativistic wind theory. It predicts that a sharp transition in jet morphology should occur with increasing radio power, as observed, and that the high luminosity jets should be fast and kinetic energy dominated. It yields the correct trend of this transition with galaxy luminosity (larger galaxies should transition at larger radio power), and is consistent with the actual value of the FR I/II break radio power, *if* the average density of accretion disk coronae in black hole ergospheres is rather low ($\sim 10^{-15} \text{ g cm}^{-3}$). The model suggests a long-term memory mechanism — the black hole spin — for assuring that radio sources maintain the same morphology over periods of time that are at least as long as the flow time from galactic center to lobe (10^{6-7} yr). In that regard, it builds on an earlier suggestion (Rees 1978) that black hole spin is the mechanism determining the *direction* of the radio jet (although the black hole spin itself may ultimately be tied to the angular momentum of mergers or collisions; see Natarajan & Pringle 1998). Because black hole rotational energy drives the radio jet, the model predicts spindown and, consequently, cosmic evolution of the FR II space density on a time scale of order 10^9 yr or less. It also suggests a possible model for radio quiet quasars (Schwarzschild black holes) and for why radio loud quasars display predominantly FR II morphology. Finally, the total amount of rotational energy liberated by the jets from a rapidly-rotating hole is more than adequate to account for the entire energy content of a typical extended radio source.

Several observational and numerical experiments have been proposed to test this model. The most important of these is the VLBI jet velocity test, in which objects with FR I morphology should have a distinctly slower ensemble-averaged jet speed than that for FR II sources. Other tests involve a similar effect for the black hole spin, a prediction for the typical density of a black hole accretion disk corona, and a search at high redshift for a population of faint extended radio sources associated with spiral or pre-spiral bulges. Proposed numerical experiments include general relativistic simulations confirming that the magnetic switch process works and that output MHD power depends critically on black hole spin.

Note added in proof: In discussing the literature on the expected power output of a rotating black hole, the author omitted an important reference. P. Ghosh & M. A. Abramowicz (1997, *Mon. Not. Royal Astron. Soc.* **292**, 887) also discussed this subject at length, assuming, as is done here, that $B_{p0} \approx B_{d0}$, and obtained expressions for the MHD power output of a rotating hole similar to those in the present paper. (Note that these authors took all of this power to be due to the Blandford-Znajek process occurring very near the horizon.) However, the absolute magnitude of their power, is about two orders of magnitude smaller than that in equation (12). Part of this difference is due to a factor of 8 in the definition of the MHD power (which was discussed by these authors), but most of

it is due to the present paper recognizing that the accretion disk can extend well interior to $6GM/c^2$ and even inside the ergosphere for rapidly rotating black holes. This yields much larger magnetic field strengths near the static limit and black hole horizon. In fact, one way in which Ghosh & Abramowicz (1997), Livio *et al.* (1999), and this paper can be brought into rough agreement is to 1) extend the disk into the ergosphere (which would increase the power computed by Ghosh & Abramowicz) and 2) treat that disk as an advection-dominated one with $H_0/R_0 \approx 1$, yielding $B_{p0} \approx B_{d0}$ (which would increase the power calculated by

Livio, Ogilvie, & Pringle).

The author is pleased to acknowledge the following: discussions with D. Jones, S. Koide, and D. Murphy; comments made by R. D. Blandford and E. S. Phinney during a seminar on this subject by the author; and helpful e-mail exchanges with E. Fomalont, C. Jackson, and R. Khanna. This research was carried out at the Jet Propulsion Laboratory, California Institute of Technology, under contract to the National Aeronautics and Space Administration.

APPENDIX

METRIC-SHEAR-DRIVEN MHD DYNAMOS

This appendix shows that shear in a general relativistic metric, like that displayed in Kerr geometry, can serve to enhance the local magnetic field strength. Magnetized plasma accreting onto a rotating black hole, therefore, will extract energy from the hole, converting it into enhanced local magnetic field strength. The effect occurs even in absence of shear in the plasma fluid flow itself and even if the magnetic field lines do not thread the black hole.

In a classical MHD flow the magnetic field evolution equation, derived from Faraday's and Ohm's laws with infinite conductivity, is

$$\frac{\partial \mathbf{B}}{\partial t} + \mathbf{v} \cdot \nabla \mathbf{B} = \mathbf{B} \cdot \nabla \mathbf{v} - \mathbf{B} \nabla \cdot \mathbf{v} \quad (\text{A1})$$

where \mathbf{B} and \mathbf{v} are the magnetic field and velocity vectors. For an initially poloidal field and rotational flow only, the ϕ component of this equation becomes, in spherical-polar coordinates,

$$\frac{\partial B_\phi}{\partial t} = r \sin\theta \left[B_r \frac{\partial \Omega}{\partial r} + B_\theta \frac{1}{r} \frac{\partial \Omega}{\partial \theta} \right] \quad (\text{A2})$$

where $\Omega \equiv v_\phi/(r \sin\theta)$ is the angular velocity field of the flow. Thus, if there is shear in a classical rotating magnetized fluid flow, a poloidal magnetic field will serve as a seed for generation of a potentially large azimuthal magnetic field that grows with time. This ‘‘omega-effect’’ is a necessary (though not sufficient) condition for an ‘‘alpha-omega’’ dynamo to exist (Roberts 1993). According to Cowling's theorem (Cowling 1934), for a full dynamo, there also must be non-axisymmetric poloidal fluid motions (due to turbulence, for example) that enhance the poloidal magnetic field as well. Such turbulent motions are thought to be a common occurrence when the rotating shear flow occurs in a gravitational field (Stone *et al.* 1996; Brandenburg *et al.* 1996). So, the presence of an omega-effect in a gravitational field is a strong indication that an alpha-omega dynamo may be operating and generating a substantial magnetosphere.

The theory of gravito-magnetic dynamos in the Kerr metric has been developed by Khanna & Camenzind (1996a), raising the possibility that even an *axisymmetric* flow can have growing, self-excited modes. Although such modes so far have not been found in kinematic numerical simulations (Brandenburg 1996; Khanna & Camenzind 1996b), the non-validity of Cowling's theorem in a general relativistic metric has been analytically confirmed by Núñez (1997), who showed that there are growing axisymmetric modes when steep gradients exist in the plasma angular velocity Ω relative to the rotating space. Here, however, we consider the simpler situation where the plasma flow itself does not shear, but there still is shear due to the general relativistic effect of frame-dragging by a rotating black hole. While this does not demonstrate the existence of a dynamo in the system, it does satisfy several of the necessary conditions for such — in particular, an omega-effect occurring in a gravitational field.

To compute the evolution of the azimuthal magnetic field, we use two different approaches — one that uses the covariant four-dimensional formalism of Misner, Thorne, & Wheeler (1973) (MTW) and one that uses the ‘‘3+1’’ decomposition of Thorne, Price, & MacDonald (1986) (TPM). Both give insight into the magnetic field enhancement process. The general relativistic analogy of equation (A1) is (Lichnerowicz 1967)

$$u^\beta B^\alpha{}_{;\beta} = B^\beta u^\alpha{}_{;\beta} - B^\alpha u^\beta{}_{;\beta} \quad (\text{A3})$$

which uses the standard MTW conventions (Einstein summation, semicolon to signify covariant differentiation, and comma for ordinary differentiation). Expanding the covariant derivatives and solving for evolution of B^α

$$\begin{aligned} u^\beta B^\alpha{}_{;\beta} &= B^\beta u^\alpha{}_{;\beta} + B^\beta u^\gamma (\Gamma^\alpha{}_{\gamma\beta} - \Gamma^\alpha{}_{\beta\gamma}) - B^\alpha u^\beta{}_{;\beta} \\ &= B^\beta u^\alpha{}_{;\beta} + B^\beta u^\gamma c_{\beta\gamma}{}^\alpha - B^\alpha u^\beta{}_{;\beta} \end{aligned} \quad (\text{A4})$$

where the $\Gamma^\alpha{}_{\beta\gamma}$ are the connection coefficients and the antisymmetric commutation coefficients are given by the components of basis vector commutators

$$c_{\beta\gamma}{}^\alpha \equiv [\mathbf{e}_\beta, \mathbf{e}_\gamma]^\alpha \quad (\text{A5})$$

The metric shear $c_{\beta\gamma}{}^\alpha$ vanishes for B^α expressed in a coordinate basis. But it does not for a physical, locally-Lorentz, orthonormal frame (one in which local observers measure physical quantities, and in which magnetic field has the units of Gauss for *all* components). In such an orthonormal frame, where we denote the coordinates with a “hat” accent, equation (A5) becomes

$$c_{\hat{\beta}\hat{\gamma}}{}^{\hat{\alpha}} = \mathcal{L}^\mu{}_{\hat{\beta}} \mathcal{L}^\nu{}_{\hat{\gamma},\mu} \mathcal{L}^{\hat{\alpha}}{}_\nu - \mathcal{L}^\mu{}_{\hat{\gamma}} \mathcal{L}^\nu{}_{\hat{\beta},\mu} \mathcal{L}^{\hat{\alpha}}{}_\nu \quad (\text{A6})$$

where $\mathcal{L}^\mu{}_{\hat{\beta}}$ is a coordinate transformation that diagonalizes the metric, converting to a locally-Lorentz system, with inverse $\mathcal{L}^{\hat{\beta}}{}_\mu$

$$\eta_{\hat{\beta}\hat{\gamma}} = \mathcal{L}^\mu{}_{\hat{\beta}} \mathcal{L}^\nu{}_{\hat{\gamma}} g_{\mu\nu} \quad g_{\mu\nu} = \mathcal{L}^{\hat{\beta}}{}_\mu \mathcal{L}^{\hat{\gamma}}{}_\nu \eta_{\hat{\beta}\hat{\gamma}}$$

To compute $c_{\hat{\beta}\hat{\gamma}}{}^{\hat{\alpha}}$, and therefore the evolution of the magnetic field for rotating black hole magnetospheres, we use the zero-charge Boyer-Lindquist version of the Kerr metric (MTW) written in the following form

$$ds^2 = -\alpha^2 dt^2 + \frac{\rho^2}{\Delta} dr^2 + \rho^2 d\theta^2 + \varpi^2 [d\phi - \omega dt]^2 \quad (\text{A7})$$

where the lapse function and angular velocity of frame dragging are given by

$$\alpha = \frac{\rho}{\Sigma} \Delta^{1/2} \quad \omega = \frac{2aMr}{\Sigma^2}$$

the various geometric functions are given by

$$\begin{aligned} \Delta &\equiv r^2 - 2Mr + a^2 & \rho^2 &\equiv r^2 + a^2 \cos^2\theta \\ \Sigma^2 &\equiv (r^2 + a^2)^2 - a^2 \Delta \sin^2\theta & \varpi &\equiv \frac{\Sigma}{\rho} \sin\theta \end{aligned}$$

$a \equiv J/M = jM$ is the specific angular momentum, and physical quantities are now in geometric units ($c = G = 1$). This metric can be diagonalized with many transformations, of course. We choose one that rotates with the same angular velocity ω as the frame-dragged space. This is the so-called Zero Angular Momentum Observer (ZAMO) system of Thorne, Price, & MacDonald (1986). The non-zero elements of this transformation and its inverse are

$$\begin{aligned} \mathcal{L}^t{}_{\hat{t}} &= 1/\alpha & \mathcal{L}^\theta{}_{\hat{\theta}} &= 1/\rho \\ \mathcal{L}^r{}_{\hat{r}} &= \Delta^{1/2}/\rho & \mathcal{L}^\phi{}_{\hat{\phi}} &= 1/\varpi \\ \mathcal{L}^\phi{}_{\hat{t}} &= \omega/\alpha & & \\ \\ \mathcal{L}^{\hat{t}}{}_t &= \alpha & \mathcal{L}^{\hat{\theta}}{}_\theta &= \rho \\ \mathcal{L}^{\hat{r}}{}_r &= \rho/\Delta^{1/2} & \mathcal{L}^{\hat{\phi}}{}_\phi &= \varpi \\ \mathcal{L}^{\hat{\phi}}{}_t &= -\varpi\omega & & \end{aligned}$$

with the $e_{\hat{r}}$ and $e_{\hat{\theta}}$ axes parallel to e_r and e_θ , respectively.

To illustrate that the metric shear acts like a fluid shear flow, consider the situation where there is no plasma motion with respect to the orthonormal system, so that the fluid four-velocity is given by $u^{\hat{\alpha}} = (-1, 0, 0, 0)$. Expressing equation (A4) in the orthonormal ZAMO frame, the evolution of the $\hat{\phi}$ component of the magnetic field, using equation (A6), is

$$\begin{aligned} B^{\hat{\phi}}{}_{,\hat{t}} &= B^{\hat{t}} c_{\hat{t}\hat{t}}{}^{\hat{\phi}} + B^{\hat{r}} c_{\hat{r}\hat{t}}{}^{\hat{\phi}} + B^{\hat{\theta}} c_{\hat{\theta}\hat{t}}{}^{\hat{\phi}} + B^{\hat{\phi}} c_{\hat{\phi}\hat{t}}{}^{\hat{\phi}} \\ &= \varpi \frac{\Delta^{1/2}}{\alpha \rho} \left[B^{\hat{r}} \frac{\partial \omega}{\partial r} + B^{\hat{\theta}} \frac{1}{\Delta^{1/2}} \frac{\partial \omega}{\partial \theta} \right] \end{aligned} \quad (\text{A8})$$

with the time and azimuthal parts vanishing. Comparing with equation (A2), then, we see that there is an exact analogy with the classical rotating fluid shear case. Any poloidal magnetic field line penetrating the space near the rotating black hole is sheared into azimuthal field at the expense of the rotational energy of the black hole, whether or not the magnetic field line actually threads the hole. This is independent of any shear in the fluid flow itself that may or may not be present.

Equation (A8) also can be derived using the “3+1” language of Thorne, Price, & MacDonald (1986) (TPM). In that case the metric equation (A7) is expressed in terms of the lapse and shift functions and a 3-metric

$$ds^2 = -\alpha^2 dt^2 + \gamma_{ij} (dx^i + \beta^i dt)(dx^j + \beta^j dt) \quad (\text{A9})$$

where γ_{ij} raises or lowers indices on the shift 3-vector β^i and 3-velocity v^i . Comparing (A7) and (A9) gives $\beta^i = (0, 0, -\omega)$, and components of (the diagonal) γ_{ij} can be determined similarly. Physical quantities like magnetic field and velocity vectors are measured in a reference frame that rotates with the ZAMOs, but they and the gradient operator ∇ are

expressed in terms of absolute (Boyer-Lindquist) spatial and time coordinates. Under these conditions, the general relativistic analog to equation (A1) is (TPM; Khanna & Camenzind (1996a))

$$\frac{\partial \mathbf{B}}{\partial t} - \mathcal{L}_\beta \mathbf{B} + \alpha \mathbf{v} \cdot \nabla \mathbf{B} = \mathbf{B} \cdot \nabla (\alpha \mathbf{v}) - \mathbf{B} \nabla \cdot (\alpha \mathbf{v}) \quad (\text{A10})$$

where \mathcal{L}_β represents the Lie derivative along β

$$\mathcal{L}_\beta \mathbf{B} = \beta \cdot \nabla \mathbf{B} - \mathbf{B} \cdot \nabla \beta \quad (\text{A11})$$

and the frozen-field condition $\mathbf{E} = -\mathbf{v} \times \mathbf{B}$ and solenoidal condition $\nabla \cdot \mathbf{B} = 0$ have been applied. We again consider the situation where there is no fluid motion with respect to the rotating space ($\mathbf{v} = 0$). Furthermore, because the gradients now are expressed in a coordinate frame, the shear terms in equation (A11) vanish, and the Lie derivative becomes simply $\mathcal{L}_\beta B^i = \beta^j B^i_{,j} - B^j \beta^i_{,j}$. As a result, the azimuthal component of equation (A10) becomes, in Boyer-Lindquist (un-hatted) coordinates,

$$B^\phi_{,t} - \beta^\phi B^\phi_{,\phi} = B^j \omega_{,j} \quad (\text{A12})$$

where $j = (r, \theta)$ only, since $\partial\beta/\partial\phi = -\partial\omega/\partial\phi = 0$. The left-hand side is proportional to the time derivative in the ZAMO frame ($= \alpha B^\phi_{,\hat{t}}/\varpi$), so transformation of equation (A12) to the locally-Lorentz orthonormal coordinates yields an equation identical to (A8). That is, even though the 3+1 formalism is expressed in the Boyer-Lindquist coordinate frame, the metric shear still is present; but that shear is now embodied in the shift vector β , rather than in the commutators $c_{\beta\gamma}^\alpha$.

Since the sheared space near a Kerr black hole is so similar in nature to that of a sheared accretion disk (*i.e.*, rotating shear flow in a gravitational field), it is likely that an instability similar to the Balbus-Hawley one also is operating. Thus, there should be not only an omega-effect enhancing the azimuthal magnetic field, but also an alpha-effect, due to the magneto-rotational-generated turbulence, enhancing the poloidal field as well. Since this process draws its energy from the hole's rotation, the strength of the magnetosphere is expected to continue to grow long after all the accretion disk's angular momentum has been removed, and to levels far greater than could be supported by the accreting matter alone.

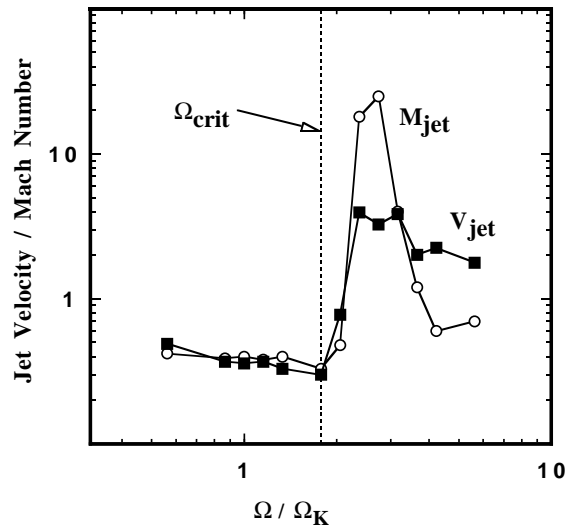
REFERENCES

- Bicknell, G. V. 1985, Proc. Astr. Soc. Austr., 6, 130.
 Bicknell, G. V. 1995, ApJS, 101, 29.
 Blandford, R. D. & Payne, D. G. 1982, MNRAS, 199, 883 (BP).
 Blandford, R. D. & Znajek, R. 1977, MNRAS, 179, 433 (BZ).
 Brandenburg, A. 1996, ApJ, 465, L115.
 Brandenburg, A., Nordlund, A., Stein, R.F. & Torkelsson, U. 1996, ApJ, 458, L45.
 Baum, S. A., Zirbel, E. L., & O'Dea, C. P. 1995, ApJ, 451, 88.
 Camenzind, M. 1989, in Accretion Disks and Magnetic Fields in Astrophysics, ed. G. Beveledere, (Dordrecht: Kluwer), p. 129.
 Cowling, T. G. 1934, MNRAS, 94, 39.
 DeYoung, D. 1976, Ann. Rev. Astr. Ap., 14, 447.
 Faber, S. M. et al. 1987, in Nearly Normal Galaxies, proc. 8th Santa Cruz Summer Wkshp on Astron. & Astrophys., (New York: Springer-Verlag), P. 175.
 Fanaroff, B. L. & Riley, J. M. 1974, MNRAS, 164, 31P.
 Hayashi, M. R., Shibata, K., & Matsumoto, R. 1996, ApJ, 468, L37.
 Henriksen, R. N. 1989, in Accretion Disks and Magnetic Fields in Astrophysics, ed. G. Beveledere, (Dordrecht: Kluwer), p. 117.
 Jackson, C. A. & Wall, J. V. 1999, MNRAS, 304, 160.
 Kellermann, K. I. et al. 1989, AJ, 98, 1195.
 Khanna, R. & Camenzind, M. 1996a, A&A, 307, 665.
 Khanna, R. & Camenzind, M. 1996b, A&A, 313, 1028.
 Koide, S., Shibata, K., & Kudoh, T. 1998a, ApJ, 495, L63.
 Koide, S., Shibata, K., & Kudoh, T. 1998b, ApJ, submitted.
 Kormendy, J. & Richstone, D. 1995, Ann. Rev. Astr. Ap., 33, 581.
 Kudoh, T. & Shibata, K. 1996, ApJ, 452, L41.
 Laing, R. A. 1996, in Energy Transport in Radio Galaxies and Quasars, eds. P. E. Hardee, A. H. Bridle, and J. A. Zensus, ASP Conf. Series Vol. 100, p. 241.
 Leahy, J. P. 1991, in Beams and Jets in Astrophysics, ed. P. Hughes, (Cambridge: Cambridge Univ. Press), p. 100.
 Ledlow, M. J. & Owen, F. N. 1996, AJ, 112, 9.
 Lichnerowicz, A. 1967, Relativistic Hydrodynamics and Magnetohydrodynamics; Lectures on the Existence of Solutions, (New York: Benjamin).
 Livio, M., Ogilvie, G. I., & Pringle, J. E. 1999, ApJ, 512, 100.
 Macdonald, D. & Thorne, K. S. 1982, MNRAS, 198, 345.
 Meier, D. L. 1976, ApJ, 207, 343.
 Meier, D. L. 1982, ApJ, 256, 681.
 Meier, D. L., Payne, D. G., & Lind, K. R. 1996, in IAU Symposium 175: Extragalactic Radio Sources, eds. R. Ekers, C. Fanti, and L. Padrielli, (Dordrecht: Kluwer), p. 433.
 Meier, D. L. 1996, ApJ, 459, 185.
 Meier, D. L., Edgington, S., Godon, P., Payne, D. G., & Lind, K. R., 1997a, Nature, 388, 350. (MEGPL)
 Meier, D. L. et al. 1997b, in IAU Colloquium 164: Radio Emission from Galactic and Extragalactic Compact Sources, eds. J. A. Zensus, G. B. Taylor, & J. M. Wrobel, ASP Conf. Series Vol. 144, p. 51.
 Misner, C. W., Thorne, K. S., & Wheeler, J. A. 1973, *Gravitation* (San Francisco: Freeman) (MTW).
 Moderski, R. & Sikora, M. 1996, MNRAS, 283, 854.
 Narayan, R. & Yi, I. 1995, ApJ, 444, 231.
 Natarajan, P. & Pringle, J. E. 1998, LANL astro-ph preprint no. 9808187.
 Novikov, I. D. & Thorne, K. S. 1973, in Black Holes, eds. C. DeWitt & B. DeWitt, (New York: Gordon & Breach), p. 343.
 Núñez, M. 1997, Phys. Rev. Lett, 79, 796.
 Owen, F. N. & Laing, R. A. 1989, MNRAS, 238, 357.
 Owen, F. N. & White, R. A. 1991, MNRAS, 249, 164.
 Punnsly, B. & Coroniti, F. V. 1990a, ApJ, 350, 518.
 Punnsly, B. & Coroniti, F. V. 1990b, ApJ, 354, 583 (PC).
 Rees, M. J. 1978, Nature, 275, 516.
 Robson, I. 1992, in Variability of Blazars, eds. E. Valtaoja and M. Valtonen, (Cambridge: Cambridge Univ. Press), p. 111.
 Romanova, M. M. et al. 1998, ApJ, 500, 703.
 Roberts, P. H. 1993, in Astrophysical Fluid Dynamics, eds. J.-P. Zahn & J. Zinn-Justin, (Amsterdam: Elsevier), p. 229.
 Schmidt, M. 1972, ApJ176, 289.
 Shakura, N. I. & Sunyaev, R. A. 1973, A&A, 24, 337.
 Sobczak, G. J., McClintock, J. E., Remillard, R. A., Bailyn, C. D., & Orosz, J. A. 199, ApJ, in press.
 Stone, J.M., Hawley, J.F., Gammie, C.F., & Balbus, S.A. 1996, ApJ, 463, 656.
 Tavani, M. et al 1996, ApJ, 473, L103.
 Thorne, K. S., Price, R. H., & Macdonald, D. A. 1986, Black Holes: The Membrane Paradigm, (New Haven: Yale Univ. Press).
 Tingay, S. J. et al. 1998, AJ, 115, 960.
 Urry, C. M. & Padovani, P. 1995, PASP, 107, 803.
 Ustyugova et al. 1999, ApJ, 516, 221.
 Vermeulen, R. C. 1996, in Energy Transport in Radio Galaxies and Quasars, eds. P. E. Hardee, A. H. Bridle, and J. A. Zensus, ASP Conf. Series Vol. 100, p. 117.
 Wall, J. V. & Jackson, C. A. 1997, MNRAS, 290, L17.
 Wilson, A. S. & Colbert, E. J. M. 1995, ApJ, 438, 62.
 Windhorst, R. A. et al 1995, Nature, 375, 471.
 Zhang, S. N., Cui, W., & Chen, W. 1997, ApJ, 482, L155.

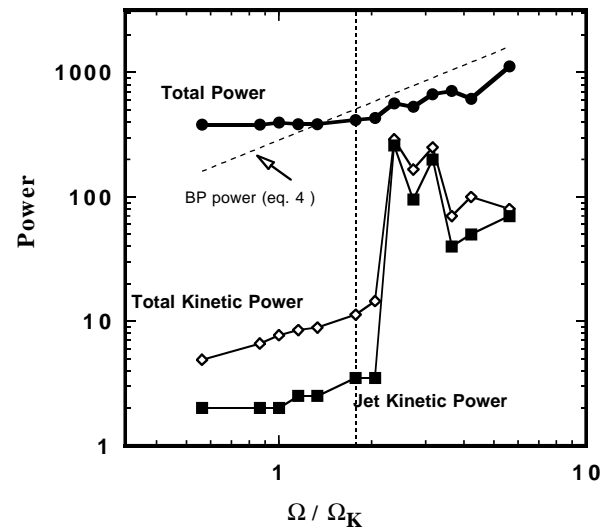
FIG. 1.— Results from 13 MHD simulations that are similar to those in MEGPL, but with angular velocity of the injected material used as the independent parameter rather than poloidal magnetic field strength. Left panel: jet velocity (filled squares) and Mach number (open circles) *vs.* angular velocity, normalized to the Keplerian value. Right panel: power output of the disk system in the form of jet kinetic power (filled squares), total kinetic power (wind plus jet, open diamonds), and total power in all forms (filled circles). For small values of Ω/Ω_K , the disk power is dominated by advected magnetic, thermal, and kinetic energy flowing into the corona (whose sum varies little or not at all with Ω). For large values of Ω/Ω_K , the disk’s magneto-rotational power (equation 4) dominates. The predicted value of Ω_{crit} (equation 6) has been modified to account for the dynamical adjustment in conditions that occurs in the injection region when $\Omega \neq \Omega_K$ (see text). When $\Omega < \Omega_{crit}$, the total power is dominated by advected magnetic energy, and the kinetic energy is dominated by that in the loosely-collimated wind. As Ω exceeds Ω_{crit} , the velocity and Mach number increase by an order of magnitude or more and the jet kinetic power becomes a substantial fraction of the total. In these non-relativistic simulations, eventually rotation becomes so fast that the flow de-collimates into a mostly radial wind.

FIG. 2.— The theoretical radio-optical plane for sub-Eddington accreting radio galaxies (left panel, $\dot{m} = 10^{-3}$) and near-Eddington accreting quasars (right panel, $\dot{m} = 1.0$). For galaxies, the optical luminosity scales roughly with the galaxy mass, as does the black hole mass. For quasars, the optical luminosity scales linearly with the black hole mass. In both cases, the radio power scales with the square of the normalized black hole spin j . Note that only the extended (unbeamed) radio power is considered here; orientation effects are ignored in these diagrams. The upper solid lines show equation (14) for a maximal Kerr hole. Middle solid lines show the theoretical FR I/FR II break (equation 17), which agrees well with the observed OLWL relation for radio galaxies (*cf.* equations 18 and 19). Lower solid lines show one measure of radio quietness (equation 26), below which the Keplerian disk MHD power dominates the ergospheric disk MHD power. Note the much smaller region spanned by FR I quasars than by FR I galaxies. FR I sources should comprise a much smaller fraction of quasars than of radio galaxies. The right panel also shows another estimate of radio quietness that makes the FR I quasar region even narrower — dashed lines where the radio to optical/UV flux ratio (1 GHz to 1 PHz) attains values of 10 and 100. The optical/UV flux was estimated by integrating the power output of a standard Shakura & Sunyaev accretion disk outward from the radius where the disk achieves an effective temperature of 10^5 K. The vertical dot-dashed line shows roughly where the optical/UV luminosity is equivalent to the stellar luminosity of a typical spiral galaxy, dividing Seyfert galaxies from quasars. As discussed in the text, the great majority of radio loud Seyferts are expected to occur only at high redshifts.

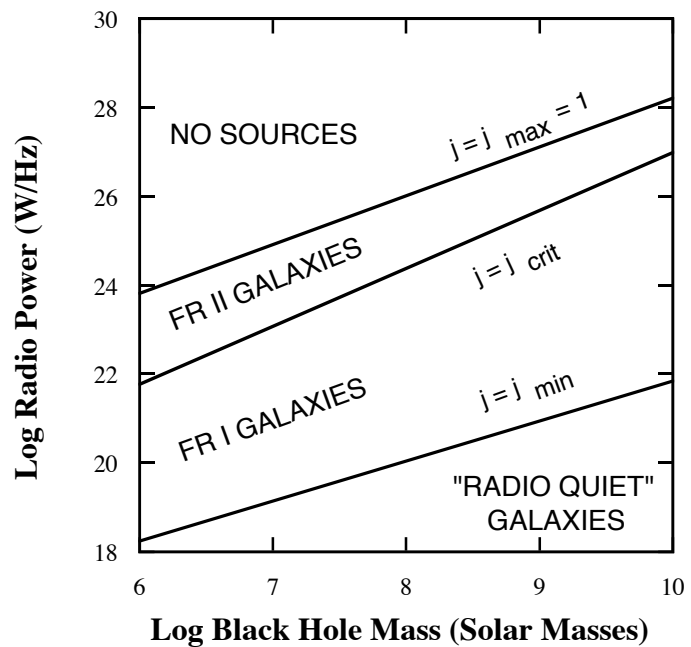
Jet Velocity and Mach Number vs. Magnetic Field Angular Velocity



Power Output vs. Magnetic Field Angular Velocity



Radio-Optical Plane (Galaxies)



Radio-Optical Plane (Quasars)

